Molecular Cell, Vol. 20, 117–129, October 7, 2005, Copyright ©2005 by Elsevier Inc. DOI 10.1016/j.molcel.2005.08.013

A Methylation-Dependent Electrostatic Switch Controls DNA Repair and Transcriptional Activation by *E. coli* Ada

Chuan He,[1,5] Jean-Christophe Hus,[1,4,5] Li Jing Sun,[1,4] Pei Zhou,[4] Derek P.G. Norman,[1] Volker Dötsch,[4] Hua Wei,[1] John D. Gross,[4] William S. Lane,[3] Gerhard Wagner,[4,*] and Gregory L. Verdine[1,2,*]

[1]Department of Chemistry and Chemical Biology
[2]Molecular and Cellular Biology
[3]Microchemistry Facility
Harvard University
12 Oxford Street
Cambridge, Massachusetts 02138
[4]Department of Biological Chemistry and Molecular Pharmacology
Harvard Medical School
240 Longwood Avenue
Boston, Massachusetts 02115

Summary

The transcriptional activity of many sequence-specific DNA binding proteins is directly regulated by posttranslational covalent modification. Although this form of regulation was first described nearly two decades ago, it remains poorly understood at a mechanistic level. The prototype for a transcription factor controlled by posttranslational modification is *E. coli* Ada protein, a chemosensor that both repairs methylation damage in DNA and coordinates the resistance response to genotoxic methylating agents. Ada repairs methyl phosphotriester lesions in DNA by transferring the aberrant methyl group to one of its own cysteine residues; this site-specific methylation enhances tremendously the DNA binding activity of the protein, thereby enabling it to activate a methylation-resistance regulon. Here, we report solution and X-ray structures of the Cys-methylated chemosensor domain of Ada bound to DNA. The structures reveal that both phosphotriester repair and methylation-dependent transcriptional activation function through a zinc- and methylation-dependent electrostatic switch.

Introduction

The transcriptional activity of sequence-specific DNA binding proteins is controlled by a wide variety of direct covalent modifications, including methylation, phosphorylation, acetylation, glycosidation, and ubiquitination (Appella and Anderson, 2001; Freiman and Tjian, 2003; Hanover, 2001; Hunter and Karin, 1992; Karin and Hunter, 1995; Sterner and Berger, 2000). This form of regulation, first discovered in the bacterial transcription factors Ada (Teo et al., 1986) and NR_I (Ninfa and Magasanik, 1986), now appears to operate throughout the biosphere. Despite their ubiquity, such regulatory systems have rarely been structurally elucidated in the modified form (Chen et al., 1998; Radhakrishnan et al., 1997); hence, the mechanistic basis for transcriptional regulation by covalent modification of transcription factors remains for the most part the subject of speculation. Here, we report the structural elucidation of the transcriptionally active form of the prototypical methylation-dependent factor *E. coli* Ada.

The integrity of the genome is constantly challenged by the presence of reactive chemical compounds in the cellular milieu. Such agents, whether they occur normally in the cell or are environmentally derived, change the covalent structure of DNA and consequently its coding properties, giving rise to mutations (Wood et al., 2001). Among the most notorious of DNA modifiers are methylating agents, which combine high mutagenic potency with widespread distribution both inside the cell and throughout the external environment. Nearly all free-standing organisms actively counter the genotoxic burden of aberrant DNA methylation by expressing proteins that search for such lesions in DNA and repair them (Friedberg et al., 1995). *Escherichia coli* exhibits the remarkable property of adapting to survive otherwise lethal dosages of methylating agents when preexposed to sublethal levels. This so-called adaptive response operates through coordinate transcriptional activation of the *ada* methylation-resistance regulon, known presently to comprise three promoters (*ada*, *alkA*, and *aidB*) that direct the expression of four proteins (Ada, AlkA, AlkB, and AidB) (Lindahl et al., 1988; Teo et al., 1986). The molecular mechanism of AidB action is unknown. AlkA is a DNA glycosylase enzyme that initiates base-excision repair of several methylated base adducts. AlkB repairs 1-methyladenine and 3-methylcytosine lesions by an oxidative demethylation mechanism (Falnes et al., 2002; Trewick et al., 2002).

Ada is a bifunctional DNA repair protein with an unusual mechanism of action. The 20 kDa N-terminal domain of Ada (N-Ada20) repairs the S_p-configurated methyl phosphotriester lesion in DNA (Figure 1A) by transferring the aberrant methyl group to one of its own cysteine residues, Cys38 (formerly thought to be Cys69; vide infra) (Sedgwick et al., 1988). As this methyl transfer is irreversible, N-Ada is not an enzyme but rather is a sacrificial, stoichiometric reagent for DNA repair. The 19 kDa C-terminal domain of Ada (C-Ada19) also uses sacrificial transfer to a cysteine residue, Cys321, in order to repair the highly mutagenic lesion O^6-methylguanine (Figure 1A) (Demple et al., 1985).

In addition to its role in repair, Ada is the key component of the chemosensory mechanism by which *E. coli* monitors its intracellular methylation burden and activates the *ada* regulon under conditions of challenge (Lindahl et al., 1988; Teo et al., 1986). The regulatory regions of *ada* regulon promoters contain a methylation-dependent activation element comprising conserved A box (AAT) and B box (GCAA) sequences separated by a six base pair spacer (Figure 1B). Unmethylated N-Ada can bind this site, but not strongly enough to activate the promoter, except when artificially overexpressed (Sakumi

*Correspondence: wagner@hms.harvard.edu (G.W.); verdine@chemistry.harvard.edu (G.L.V.)
[5]These authors contributed equally to this work.

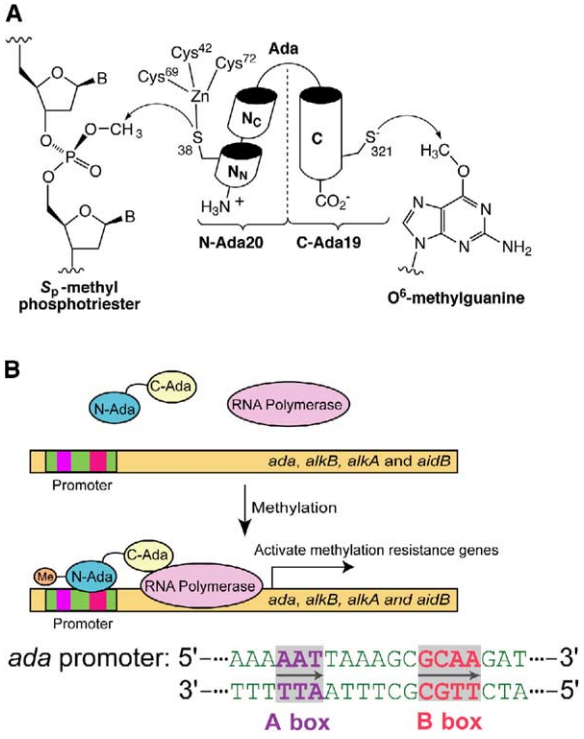

Figure 1. DNA Repair and Transcriptional Activation by *E. coli* Ada

(A) Domain organization of *E. coli* Ada, and DNA repair reactions performed by each domain.

(B) Overview of transcriptional activation. Methylation of Cys38 increases by 10^2- to 10^3-fold the strength of sequence-specific DNA binding by Ada, thereby enabling the protein to bind the promoters of the *ada* regulon and activate four genes: *ada*, *alkB*, *alkA*, and *aidB*. The sequence at the bottom is that of the Ada binding site in the *E. coli ada* promoter, with the conserved A box and B box elements in purple and fuchsia, respectively, and unconserved positions in green. Arrows embedded in the sequence denote the orientation of the A box and B box with respect to the start point of transcription.

and Sekiguchi, 1989). Transfer of a methyl group to Cys38 increases dramatically the affinity of the protein for DNA (Myers et al., 1995a), enabling it to stably bind *ada* regulon promoters and recruit RNA polymerase for the initiation of transcription (Akimaru et al., 1990; Landini and Busby, 1999; Landini and Volkert, 1995a). It remains to be understood how the addition of one methyl group to N-Ada can bring about such a pronounced gain of biological function.

Biochemical studies on N-Ada20 have revealed that it possesses two constituent domains, N-Ada_N (residues 1–75) and N-Ada_C (residues 78–178), connected by a flexible linker (Figure 1A). Whereas both domains are required for sequence-specific DNA binding, N-Ada_N alone is fully capable of repairing S_p-configurated methyl phosphotriesters in DNA (Myers et al., 1992; Sakashita et al., 1993). N-Ada_N contains a Zn^{2+} ion tightly coordinated to four Cys residues (Cys38, Cys42, Cys69, and Cys72) (Myers et al., 1993). The metal does not merely serve a structural role, however, as one of its ligands is Cys38, the nucleophilic methyl acceptor residue (see below); indeed, the bound metal ion is required to activate the nucleophilicity of Cys38 (Myers et al., 1993). Ada is the prototype for an emerging group of proteins that use zinc-coordinated thiol groups as nucleophiles in alkyl group transfer reactions. More recent examples include cobalamin-dependent and -independent methionine synthase, protein farnesyltransferase (FTase), and geranylgeranyltransferase (GTase) and possibly methanogenic methyl transferases and epoxide carboxylase (Allen et al., 1999; Hightower and Fierke, 1999; LeClerc and Grahame, 1996; Matthews and Goulding, 1997).

Developing a complete picture of metalloactivated DNA repair and methylation-dependent transcriptional activation by Ada has not been possible in the absence of high-resolution structural information on the methylated N-terminal domain bound to DNA. In this report, we describe two high-resolution structures of N-Ada bound to DNA: one determined by X-ray and the other by NMR. Together, these structures reveal significant insights into several major aspects of Ada function: the mechanism of Cys38 metalloactivation, the origins of S_p-stereospecificity in methyl phosphotriester repair, the basis for methylation-dependent enhancement of DNA binding, and the commonality in features of DNA repair and sequence-specific DNA binding. The structures reveal that Ada uses a unique electrostatic switching strategy to target methyl phosphotriesters and promoters of the *ada* regulon.

Results and Discussion

Overall Structure

Details of sample preparation, crystallization, NMR data collection, and structure determination are provided in the Experimental Procedures. Statistics for data collection and structure determination are summarized in Table 1 (X-ray) and Table 2 (NMR).

The overall structure of the N-Ada-DNA complex is similar in the X-ray (Figure 2A) and NMR (Figure 2B, see Figure S1, available in the Supplemental Data with this article online, for a stereo view of the ensemble) structures. The protein contains two domains, N-Ada_N (residues 9–75) and N-Ada_C (residues 80–138), connected by a flexible linker (residues 76–79). N-Ada_N folds into a globular domain having a central β sheet sandwiched between α helices, with the zinc ion being bound at one edge of the sheet; the overall fold and zinc-coordination motif of N-Ada_N are similar to those observed in the solution structure of this domain alone in the absence of DNA (Lin et al., 2001; Myers et al., 1993) but have no counterpart in any other known protein. N-Ada_C folds into an α-helical domain similar to that found in the Rob (Kwon et al., 2000) and MarA (Rhee et al., 2000) transcription factors. The two domains of N-Ada lie along one face of the DNA helix, such that the long axes of the protein and DNA are parallel.

In the NMR structure, N-Ada_N is bound over the minor groove of the A box and N-Ada_C inserts the recognition helix of its canonical helix-turn-helix motif (Dodd and Egan, 1990) into the major groove of the B box (Figure 2B). As discussed in greater detail below, this recognition mode is consistent with biochemical data on DNA recognition by N-Ada, hence, we conclude that the solution structure represents that of a

Table 1. X-Ray Data Collection, Structure Determination, and Refinement Statistics

Crystal	SeMetλ1[a]	SeMetλ2	SeMetλ3
Wavelength (Å)	0.9794	0.9797	0.9537
Resolution (Å)	50–2.1 (2.18–2.10)	50–2.1 (2.18–2.10)	50–2.1 (2.18–2.10)
R_{sym}[b]	0.072 (0.474)	0.072 (0.496)	0.077 (0.535)
Total number of observations	180,647	177,930	172,340
Number of unique observations	27,183 (1936)	27,095 (1788)	26,922 (1587)
Completeness	91.3 (64.7)	90.2 (59.8)	89.1 (52.3)
I/σ (I)	22.7 (2.1)	22.9 (1.9)	20.6 (1.6)
Number of sites	3	3	3
Phasing power (acentric/centric)[c]	2.04/2.37	2.11/2.51	1.16/1.41
R_{cullis} (ano)[d]	0.60	0.58	0.78
Space group	$P2_12_12_1$		
Number of nonhydrogen atoms	1,814		
Number of water molecules	92		
$R_{working}$[e] (%)	0.235		
R_{free} (%)	0.274		
Average B factor	35.32		
Rmsd bonds (Å)	0.006		
Rmsd bonds (°)	1.1		
Ramachandran distribution[f]			
Most favorable region: 93.9%	Additionally allowed region: 6.1%	Generously allowed region: 0.0%	Disallowed region: 0.0%

[a] Dataset used in refinement.
[b] R_{syn} is the unweighted R value on I of symmetry-related reflections ($\Sigma_{hkl}|I_{hkl} - \langle I_{hkl}\rangle|/(\Sigma_{hkl}I_{hkl})$.
[c] Phasing power is the rms of the heavy atom structure factor amplitudes divided by the rms of the residual lack of closure error.
[d] R_{cullis} is the mean lack of closure error divided by the isomorphous difference.
[e] $R_{working} = \Sigma_{hkl}|F_{obshk} - F_{calchkl}| / \Sigma_{hkl}|F_{obshkl}|$, R_{free} is calculated from 5% of reflections not used in model refinement.
[f] Determined using PROCHECK (Laskowski et al., 1993).

fully sequence-specific complex. The 18-mer oligonucleotide adopts a conformation representative of B-DNA. The nuclear Overhauser effect (NOE) walk-through patterns from both the aromatic to H2′/H2″ and aromatic to H1′ observed are consistent with B-DNA structure.

Whereas the X-ray structure reveals an N-Ada_N-A box interface quite similar to that in solution, the N-Ada_C-B box interface differs markedly in the two structures. This difference can be ascribed to an unusual packing mode observed in the X-ray structure. Even though the 17-mer oligonucleotide used in the crystallization contains intact A and B box sequences from the *ada* promoter and forms a strong 1:1 complex with methylated N-Ada in solution (data not shown), the protein does not bind the 17-mer in the conventional mode observed in solution (compare the gray shaded sequences in Figure 2). Instead, in the crystal, N-Ada_N is bound to a different A box sequence fortuitously present in the *ada* promoter. The midriff of the protein straddles over two duplexes that are coaxially stacked in the crystal, thereby presenting N-Ada_C to a nonspecific sequence located on the neighboring DNA molecule (Figure 2A). The interactions between N-Ada_N and the phosphodiester backbone of the A box in the crystal structure correspond precisely to the phosphate contacts inferred from ethylation interference footprints of methylated N-Ada bound sequence specifically to the *ada* and *alkA* promoters (J. Liu and G.L.V., unpublished data), indicating that methylated N-Ada_N is bound sequence specifically to the A box in the crystal. Conversely, the paucity of specific contacts between N-Ada_C and DNA reveals that the two are bound nonsequence specifically in this segment of the crystal structure. The 17-mer duplex oligonucleotide adopts a B-DNA conformation throughout, without any significant distortions. The two ends of the DNA are coaxially stacked to form a pseudo-continuous helix, with the unpaired nucleotides swung out to an extrahelical position. The only noteworthy deviation from a canonical B-form duplex occurs at the junction, where the helix is twisted by only ~10° instead of the usual ~30°, such that the long axes of base pairs 5 and –12 are nearly parallel (Figures 2A and 3C).

Although the overall features of N-Ada_N-A box recognition are clearly similar in the X-ray and NMR structures, the paucity of NOE data for the head groups of amino acid side chains, especially Arg, does not allow us to assign intermolecular contacts unambiguously. Therefore, the analysis that follows will draw primarily upon the X-ray structure for detailed analysis of sequence-specific A box recognition. The solution structure, on the other hand, provides an ample basis for understanding specific N-Ada_C-B box interactions.

A Box Recognition

N-Ada_N grasps the backbone of the noncoding DNA strand, making extensive hydrogen bonding contacts to phosphate groups on this strand by using both side chains and main-chain amides of the protein (Figure 3A). These backbone interactions position the domain over DNA so as to present two basic residues, Arg45 and Arg71, to the bases of the minor groove. Arg45, which is borne on a long loop known to be involved in DNA recognition (Myers et al., 1993), inserts its guanidinium head group into the minor groove of the A box and hydrogen bonds to thymines T2 and T3 (see Figure 2A for numbering, Figure 3B). This positioning of Arg45 would be sterically incompatible with a G at any position in base pairs 2 and 3, thereby explaining the preference of the protein for A/T pairs at these positions. The

Table 2. Statistics for the Solution Structure of Methylated N-Ada-DNA Complex

Protein	
Amino acids residues sequentially assigned (nonproline)	125 of 131
Effective distance constraints[a]	1431
Intraresidue	483
Sequential (|i–j| = 1)	388
Medium range (|i–j| $\leq$ 4)	226
i, I + 2	90
i, I + 3	66
i, I + 3	70
Long range (|i–j| $\geq$ 5)	264
H bonds	70
Dihedral angle constraints[a]	416
DNA	
Effective distance constraints[a]	376
Intraresidue	150
Sequential	139
H bond	87
Protein-DNA Interface	
Effective distance constraints[a]	22
Rmsd to the mean for backbone heavy atoms of all secondary structure elements (Residues 9–17, 27–31, 36–39, 51–55, 58–63, 68–70, 80–94, 102–108, 114–123, and 129–139)	0.84
Rmsd to the mean for heavy atoms of all secondary structure elements (Residues 9–17, 27–31, 36–39, 51–55, 58–63, 68–70, 80–94, 102–108, 114–123, and 129–139)	1.23
Rmsd to the mean for backbone heavy atoms (Residues 8–139)	0.87
Rmsd to the mean for heavy atoms (Residues 8–139)	1.26
Rmsd to the mean for DNA heavy atoms (Superposition of all DNA heavy atoms)	0.22
Rmsd to the mean for protein + DNA heavy atoms (Superposition of all secondary structure elements heavy atoms and DNA heavy atoms)	0.96
Ramachandran plot[b]	Residues 1-139
Most favorable region: 94.5%	Additionally allowed region: 5.5%
Generously allowed region: 0.0%	Disallowed region: 0.0%

[a] Redundant distance constraints are removed by DYANA. Effective distance constraints were used to generate the statistics.
[b] Determined using PROCHECK.

basis for the A/T preference at the first position of the A box (A1/T1) is not apparent from our structures. The main chain amide NH group of Arg45 also makes water-mediated hydrogen bonds to the base pair just outside the A box on the 3′ side (A4/T4). The side-chain guanidinium group of Arg71 hydrogen bonds in the minor groove to two thymines located at opposite ends of the DNA duplex (T5 and T-12, Figure 3C). In the crystal, the T5 and T-12 residues on neighboring duplexes are brought together by coaxial stacking, and we envision that Arg71 may help to stabilize such packing of the DNA. Although the sequence of the spacer is not strictly conserved among the known Ada binding sites in the *ada*, *alkA*, and *aidB* promoters, it is A/T rich in all three instances (Landini and Volkert, 1995b), suggesting perhaps that the Arg71 contact makes a valuable contribution to promoter recognition by Ada.

B Box Recognition

The C-terminal domain of N-Ada contains a canonical helix-turn-helix motif (HTH, α-D and α-E), the recognition helix of which (Figures 4A and 4B; α-E) inserts into the major groove of the B box to make sequence-specific base contacts. In the solution structure, the aryl ring of Phe114 contacts the methyl groups of both T12 and T13, as evidenced directly by interfacial NOEs. The calculations indicate that the guanidinium group of Arg118 hydrogen bonds to the O^6 atoms of both G10 and G11, though the absence of NOEs to the guanidinium head group does not permit an unambiguous contact assignment. The identities of the bases in the B box contacted by N-Ada_C inferred from the solution structure correspond exactly to those determined independently by a biochemical method, template-directed interference (TDI) footprinting (Storek et al., 2002). Interestingly, the solution structure also positions His115 to hydrogen bonding to a base outside the B box on its 5′ flank, C9. The existence of this contact has been confirmed by the observation of interference at C9 in TDI footprints of the *ada* promoter (Storek et al., 2002). This interaction of His115 to C9, a nonconserved base, may explain the 10-fold higher affinity of N-Ada for the *ada* promoter versus the *alkA* and *aidB* promoters, which have an A base at the equivalent position (Landini and Volkert, 1995b). Several other residues of the HTH motif, the loop on its C terminus, and the α-F helix make phosphate contacts to the DNA backbone.

Comparison of the solution and X-ray structures of N-Ada_C reveals a nearly identical overall fold (Figure 4A). However, the disposition of the N-Ada_C domain with respect to DNA in the two structures is markedly different, thus suggesting that a domain shift accompa-

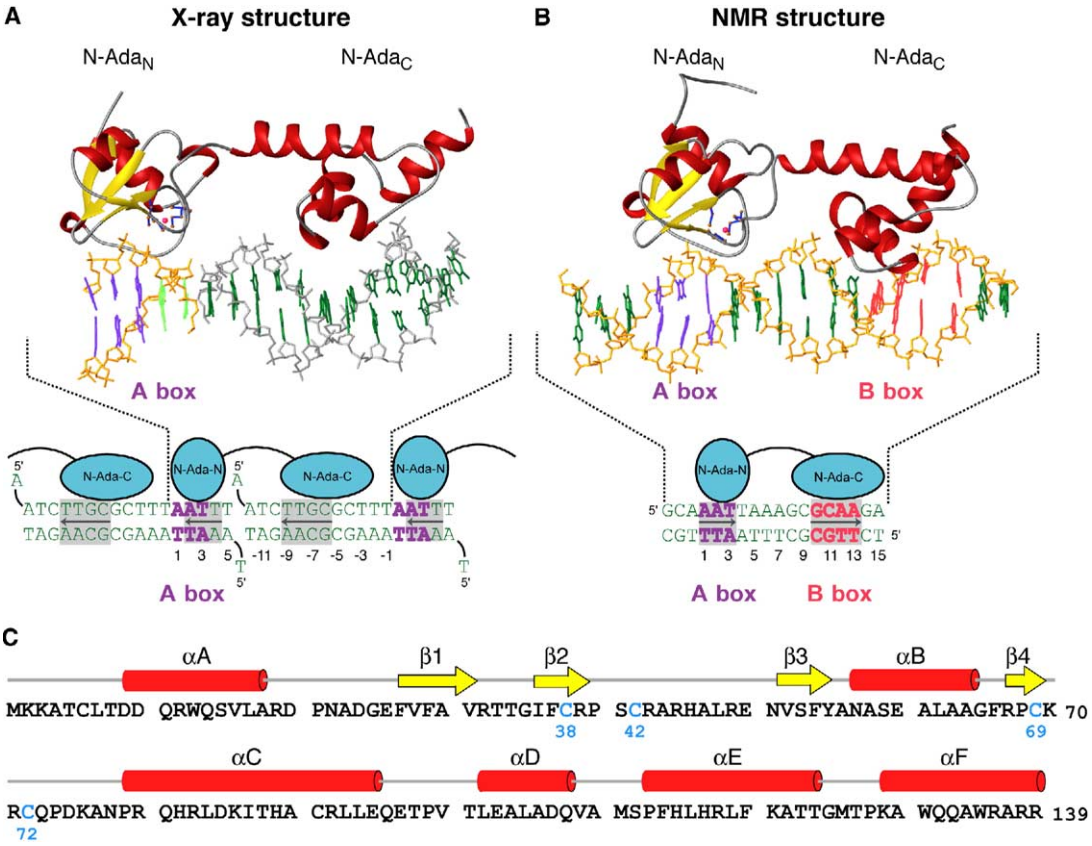

Figure 2. Overall Views of the Crystal (X-Ray) and Solution (NMR) Structures

(A) In the X-ray structure, the Cys38-methylated N-Ada$_N$ domain is bound specifically over an A box sequence (purple) fortuitously present in the oligonucleotide, and the N-Ada$_C$ domain jumps over the helix packing interface to contact a nonspecific sequence located on the adjacent duplex in the crystal. Note that the oligonucleotide contains an intact Ada binding site from the *ada* promoter (A box and B box shaded with arrows as in Figure 1), but the protein is not bound to these sequences in the crystal. The color code for the DNA of the top figure is as follows: purple, A box; light green, nonspecific DNA at one end of the duplex; and dark green, nonspecific DNA comprising the rest of the oligonucleotide. The unpaired A and T overhangs at the helix junction are disordered and therefore are not shown.

(B) In the solution structure, N-Ada$_N$ is bound specifically to the A box (purple) and N-Ada$_C$ is bound specifically to the B box (fuchsia). Noncognate sequences are in dark green. Note the orientation of the protein over the A and B boxes, with the arrows pointing toward the start point of transcription; comparison with (A) reveals an inverted binding mode in the latter.

In (A) and (B), the side chains of the zinc-ligand residues are visible in the N-Ada$_N$ domain, with the zinc ion represented by a pink sphere.

(C) Sequence and secondary structure of truncated N-Ada proteins used in this study, with α helices depicted as red cylinders and β strands as yellow arrows, according to the color scheme in (A) and (B). The four Cys residues that coordinate zinc are colored blue.

nies the transition from a sequence-specific (Figure 4A, red) to a nonspecific (cyan) binding mode. In the X-ray structure, the entire N-Ada$_C$ domain is retracted from the DNA surface, such that the recognition helix of N-Ada$_C$ is not in position to make base-specific contacts but instead interacts extensively with the DNA backbone. Only one base-specific interaction is evident, that between Phe114 and the methyl group of T8. The general features of domain retraction and replacement of direct phosphate contacts have also been observed in comparisons of the specific versus nonspecific binding modes of the glucocorticoid hormone receptor (Luisi et al., 1991), BamHI endonuclease (Viadiu and Aggarwal, 2000), and *lac* repressor (Kalodimos et al., 2004). It is envisioned that the relatively loose association of the domain with DNA, mediated largely by favorable charge-charge interactions, may provide an efficient means for the protein to slide along DNA while translocating from non-specific to specific sites.

Identity of the Methyl Acceptor Residue

Prior to crystallization, N-Ada had been methylated by treatment with methylphosphotriester-containing DNA. On the basis of previous biochemical studies (Sedgwick et al., 1988), we expected to find a methyl group on Cys69, the putative acceptor residue. Despite the high quality of the electron density maps in the region around the (Cys$_4$)Zn center, these maps did not show any extra density on Cys69 consistent with the presence of a covalently attached methyl group. On the other hand, we did observe extra electron density protruding from the sulfur atom of Cys38, and into this space a methyl group could be modeled with good geometry and high (97%) occupancy (Figure 5A).

To obtain an independent determination of the location of the methyl group added posttranslationally to Ada, we prepared samples of N-Ada methylated by treatment with double-stranded or single-stranded DNA containing a single methyl phosphotriester or by treat-

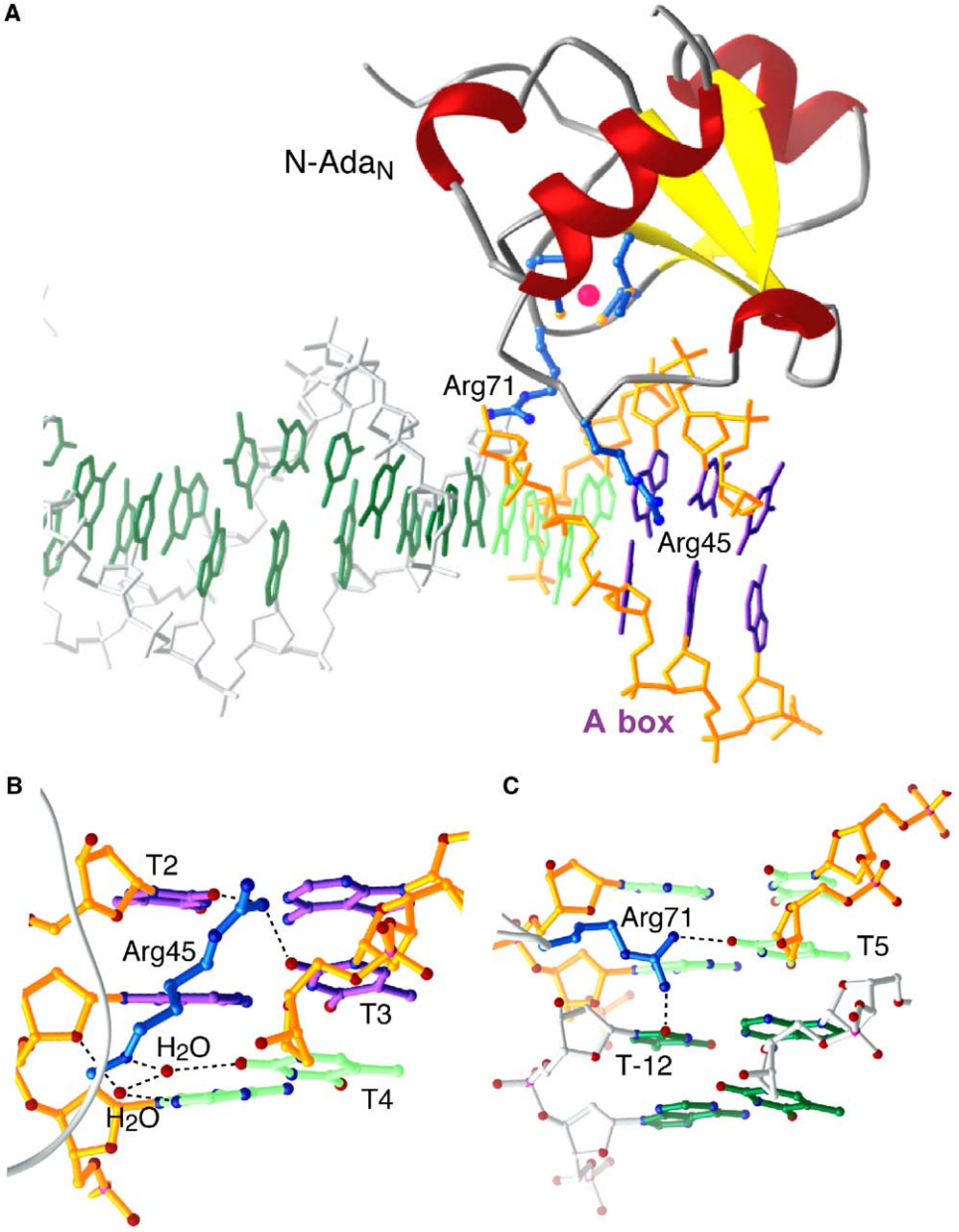

Figure 3. Contacts between N-Ada$_N$ and DNA

(A) View of the N-Ada$_N$ domain alone from the crystal structure, bound over the full-length DNA. The side chains of the ligand residues for the zinc ion (pink) are shown explicitly. Two Arg residues that make important contacts, Arg45 (interacting with A box) and Arg71, are also shown.

(B and C) Close-up views of the contacts between the DNA minor groove and Arg45 (B) and Arg71 (C). Color coding of the DNA is identical to that in Figure 2A, with the A box fortuitously present in purple.

ment with CH_3I, a known gratuitous inducer of the adaptive response. The precise site of methylation in these protein samples was then identified by microcapillary LC-MS/MS. Regardless of the methylating agent employed, MS/MS of tryptic peptides identified the peptide $_{33}$TTGIFC(Me)RPSCR$_{43}$ to be uniquely methylated at the cysteine corresponding to Cys38. A synthetic peptide made with this modification produced an identical fragmentation spectrum (see Figure S2). No methylation was detected at this site in untreated N-Ada when similarly prepared and analyzed. Sequencing of the tryptic peptide $_{50}$ENVSFYANASEALAAGFRPCK$_{70}$ spanning Cys69 in each of the treated samples revealed no methylation at this residue. These results provide unambiguous biochemical evidence in support of Cys38 as the active-site cysteine nucleophile of N-Ada.

Further confirmation for Cys38 as the methyl acceptor residue comes from the NMR data. The posttranslationally added methyl group shows a strong NOE to Phe29, even at short mixing times, indicating a close

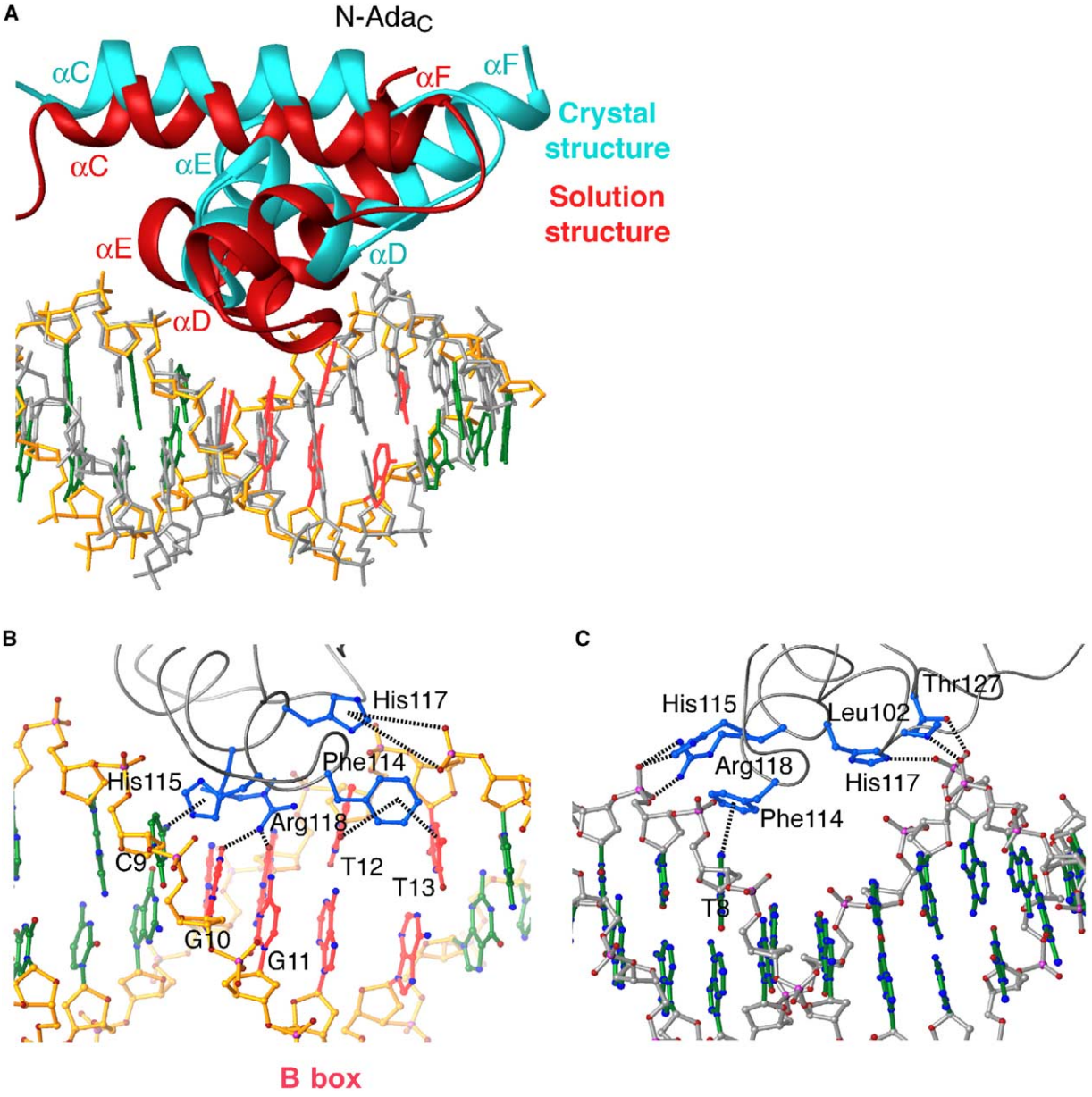

Figure 4. Contacts between N-Ada$_C$ and DNA

(A) Least-squares superposition of the N-Ada$_C$-DNA interface, with the DNA as reference point. The coloring of the DNA is as in Figures 2A and 2B (B box is in red); N-Ada$_C$ from the crystal structure is in blue; solution structure, red.

(B) Interface between the B box and N-Ada$_C$ in the solution structure.

(C) Interface between the B box and N-Ada$_C$ in the crystal structure. Note the multiple base-specific contacts in Figure 4B, in contrast with the preponderance of backbone contacts in Figure 4C.

distance relationship between these two moieties. A methyl group placed on Cys69 is too remote from Phe29 to be consistent with the observed NOE (refer to Figure 5B). On the other hand, a methyl group on Cys38 lies within van der Waals contact distance of the Phe29 aryl ring, in full concordance with the NOE data. Furthermore, the overall fit of the solution structure to the experimental data is significantly better when the methyl group is placed on Cys38 than on Cys69.

Based on the three independent lines of evidence cited above—X-ray, MS/MS sequencing, and NOE data—we conclude that Cys38 of Ada, and not Cys69 as previously believed, is the zinc bound Cys residue that removes methyl groups from the DNA backbone.

Active Site Structure and Chemistry

Of long-standing interest has been the mechanisms by which Ada (1) directs the regiochemistry of methyl transfer to just one of its four zinc bound Cys residues, (2) obtains stereochemical specificity for S_p-configur-

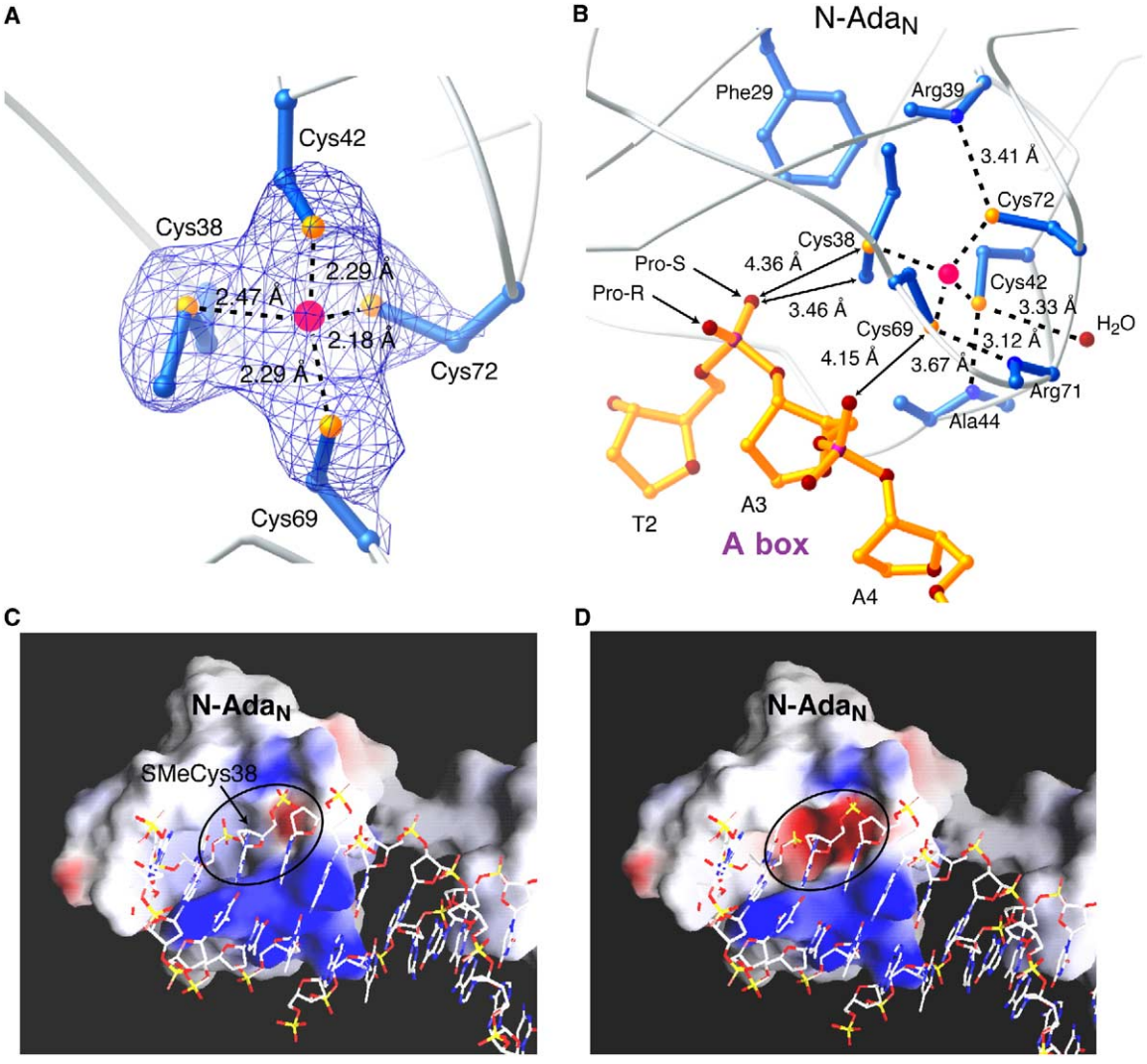

Figure 5. Mechanism of Ada

(A) Close-up view of metal coordination in the crystal structure of N-Ada bound to DNA. The metal is shown as a pink sphere, and the side chains of the ligand residues are cyan, with sulfur atoms colored yellow. The map represents simulated annealing omitting the Zn^{2+}, the four sulfur atoms of the ligand residues and the posttranslationally added methyl group ($F_{obs} - F_{calc}$, 2σ). Note the presence of density corresponding to the methyl group at the position of Cys38 and the absence of density at Cys69.

(B) Close-up view of the interface between Cys38-methylated N-Ada$_N$ and the A box, with relevant distances and identities of residues denoted.

(C and D) Electrostatic surface (GRASP; Nicholls et al., 1991) representations of N-Ada$_N$ in the Cys38-methylated state (C) and unmethylated state ([D], modeled by removal of the Cys38 methyl group from the X-ray structure in silico). Red, negatively charged surfaces; blue, positively charged surfaces; and white, neutral. Note the change in charge state of the prominent pocket into which the DNA backbone binds, from net negative (repulsive) in (D) to nearly neutral in (C).

ated methyl phosphotriesters, and (3) gains a factor of 10^2–10^3 in the strength of sequence-specific DNA binding by the acquisition of a single methyl group. The data presented here, in particular the high-resolution X-ray structure, shed significant light on each of these issues.

The phosphotriester repair function of the Ada protein is contained entirely within N-Ada$_N$ (Myers et al., 1992). In the X-ray structure, the active site of N-Ada$_N$ is clamped directly over the phosphodiester backbone of the noncoding strand of the A box (Figure 5B). The four zinc ligand residues adopt a distorted tetrahedral arrangement about the Zn^{2+}, with the three Cys thiolates (Cys42, Cys69, and Cys72) having roughly equal metal-ligand bond distances (2.18–2.29 Å), and the SMeCys38 thioether sulfur ligand having a significantly elongated bond to the Zn^{2+} (2.47 Å). These metal-ligand distances are well within expectation, based on the corresponding distances observed in small-molecule coordination complexes (Berreau et al., 2000; Clark-Baldwin et al., 1998). The structural data are also in general accord with EXAFS measurements on methylated N-Ada bound specifically to DNA, which indicate the presence of three thiolate ligands having average

bond distances of 2.32 Å and a thioether ligand with a distance of 2.52 Å (Lin et al., 2001). The elongation of the Zn^{2+}-SMeCys38 bond can be understood straightforwardly as resulting from the weaker Zn^{2+}-thioether interaction than with a Zn^{2+} thiolate. The relatively weak coordination of Zn^{2+} to thioether ligands is believed to explain why no known native Zn^{2+} binding protein uses a Met residue as a ligand. In fact, Cys38-methylated N-Ada is exceedingly prone to denaturation in the absence of DNA but is stable in the presence of DNA, presumably because the protein-DNA interaction stabilizes the otherwise labile coordination of the SMeCys38 thioether ligand to the Zn^{2+}.

The observation that methyl iodide regiospecifically methylates Cys38 while leaving the other three zinc bound Cys residues unaffected (Myers et al., 1995b) indicates that the Cys38 thiolate is selectively activated as a nucleophile. The basis for this selective activation can be understood from inspection of the X-ray structure. Whereas the thiolate sulfur atoms of Cys42, Cys69, and Cys72 are engaged in hydrogen bonding interactions to backbone amide NH groups and an ordered water molecule, SMeCys38 is free of any such hydrogen bonding interactions. Zinc bound thiolates exhibit an intrinsically high reactivity as nucleophiles (Wilker and Lippard, 1997), and this reactivity is suppressed by hydrogen bonding. Zinc bound thiolates in metalloproteins are frequently hydrogen bonded to backbone amides, both to suppress their reactivity and to stabilize their metal coordination by alleviating electrostatic repulsion with neighboring ligands (Blake et al., 1992; Maynard and Covell, 2001). These thiolate/amide hydrogen bonds can be strong enough to have significant covalent character, as evidenced by the fact that they often exhibit scalar coupling in NMR spectra (Blake et al., 1992). Consistent with this notion, density function theory calculations indicate that amide-Cys hydrogen bonding can decrease the basicity of the metal bound thiolate by as much as 14 pK_a units (Maynard and Covell, 2001). Notwithstanding these considerations, it remains a formal possibility that Cys38 is hydrogen bonded in the unmethylated state, but not in the methylated state. This explanation is inconsistent with the X-ray structure, however, because there is simply no suitable candidate for a hydrogen bond donor in the vicinity of SMeCys38. Steric accessibility does not appear to play a significant role in the selective activation of Cys38, because Cys69 is also surface exposed yet is not methylated by methyl iodide (Myers et al., 1995b). Based on the available data, the most reasonable model is one wherein Ada dampens the nucleophilicity of Cys42, Cys69, and Cys72 through hydrogen bonding while maintaining the intrinsically high nucleophilicity of the Cys38 thiolate by keeping it free from hydrogen bonding interactions.

The Stereochemistry of Methyl Transfer

The stereochemical specificity of Ada to repair only S_P-configurated methyl phosphotriesters in DNA can be rationalized on the basis of the structure. The sulfur atom of SMeCys38 projects directly toward the pro-S oxygen atom of the phosphate located between T2 and A3 (T2pA3). Indeed, the methyl group of SMeCys38 is located only ~3.5 Å away from the pro-S oxygen, such that one can readily envision in-line S_N2 transfer of a methyl group from the pro-S oxygen atom to the Cys38 thiolate sulfur atom (Figure 5B). Conversely, the pro-R oxygen on T2pA3 is too far away from Cys38 (5.0 Å from pro-R oxygen to methyl carbon of SMeCys38) and is pointed in the wrong direction to allow in-line methyl transfer.

Methylation-Dependent Enhancement of DNA Binding

Since the discovery that methylation of Ada is the signal that induces activation of the *ada* regulon, a mystery has been how such a minor change in the protein structure can engender such a profound gain of biological function. The prevailing hypothesis has held that methylation triggers some sort of structural rearrangement, which in turn unveils a previously masked DNA-recognition interface in the protein. The present structures conclusively rule out any such allosteric modulation, because the overall fold of methylated N-Ada_N in complex with DNA is virtually the same as that in the unliganded, unmethylated form. Inspection of the complex structures suggests an alternative mechanism, based on electrostatic switching, for the methylation-dependent enhancement of DNA binding by Ada.

The X-ray structure reveals that N-Ada_N docks with DNA so as to present two of its zinc-coordinated Cys residues (Cys38 and Cys69) to two successive phosphate groups on the DNA (T2pA3 and A3pA4, Figure 5B). The sulfur atom of SMeCys38 is only 4.36 Å removed from the pro-S oxygen of T2pA3, whereas the sulfur atom of Cys69 is only 4.15 Å away from the pro-S oxygen of A3pA4. In this configuration, electrostatic repulsion between the phosphate oxygens and thiolate sulfur atoms is expected to influence profoundly the strength of the overall protein-DNA interaction. In the absence of a methyl group on Cys38, each thiolate sulfur bears 1/2 negative charge and would have to approach an oxygen atom also bearing 1/2 negative charge (Figure 6A). Methylation on Cys38 eliminates the charge on this sulfur atom and also reduces the fractional charge on Cys69 to 1/3 negative (Figures 6C and 6D). Thus, to a first approximation, methylation reduces the overall extent of charge/charge repulsion in the protein-DNA interface by 2/3 of a negative charge. The structure suggests a further reduction in repulsive charge-charge interactions may be made by the methyl group on Cys38 screening T2pA3 from the negative charge on Cys42 (refer to Figure 5B). The effect of methylating Cys38 can be visualized from the electrostatic surface charge distribution of N-Ada in the presence (Figure 5C) and absence (Figure 5D) of a methyl group on Cys38. Simple removal of a methyl group from the X-ray structure reveals that the pocket into which the DNA backbone binds has a negatively charged surface (Figure 5D). The extent of negative charge is dramatically reduced by methylation of Cys38 (Figure 5C).

If alleviation of electrostatic repulsion is indeed responsible for the methylation-dependent enhancement of DNA binding by Ada, then alternative modifications of the protein-DNA interface that reduce these repul-

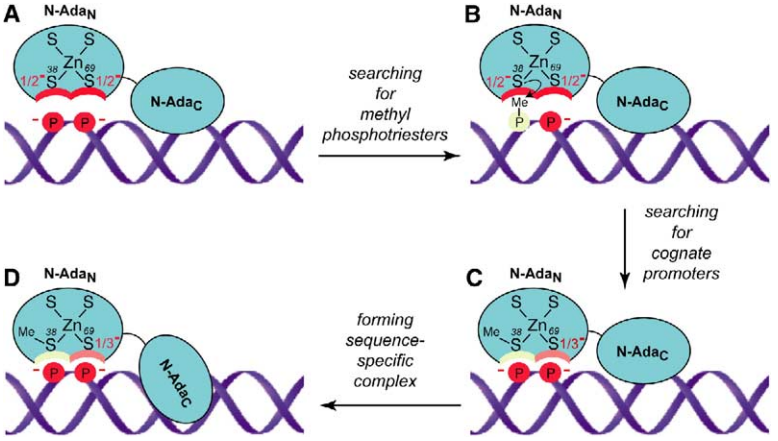

Figure 6. Control of DNA Phosphotriester Repair and Transcriptional Activation by a Metal-Mediated Electrostatic Switch

Circles denote successive phosphates in DNA, which are either negatively charged as phosphodiesters (red) or neutral as the phosphotriester (yellow). The zinc coordination sphere of N-Ada$_N$ is illustrated schematically with Cys38 and Cys69 in close juxtaposition to successive phosphates. The net charges indicated on Cys38 and Cys69 (the other two Cys residues bear the same net charge as Cys69) were calculated by assuming (1) that all zinc-coordinated Cys residues bear –1 formal charge, the metal bears +2 formal charge, and the zinc-coordinated thioether is charge neutral; and (2) the same net charge is spread over all zinc-coordinated Cys thiolates. A red stripe on N-Ada$_N$ denotes a negatively charged surface, and yellow indicates a neutral surface. A detailed explanation of the model is given in the text.

sions should similarly stimulate DNA binding. To test this notion, we incorporated the neutral N-methyl phosphoramidate linkage at positions T2pA3 and A3pA4 and at remote location from outside the Ada binding site. The affinity of unmethylated Ada for these methylated oligonucleotides was measured by electrophoretic mobility shift assays (Figure 7). Introducing a neutral

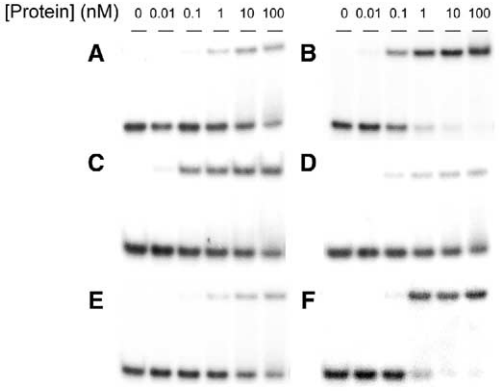

	Protein	DNA	Kd (nM)
A	N-Ada16Δ	CAGCGAAAAAAATTAAAGCGCAAGATTGTTGG GTCGCTTTTTTTTAATTTCGCGTTCTAACAACC	1.3
B	Methylated N-Ada16Δ	CAGCGAAAAAAATTAAAGCGCAAGATTGTTGG GTCGCTTTTTTTTAATTTCGCGTTCTAACAACC	0.014
C	N-Ada16Δ	CAGCGAAAAAAA TTAAAGCGCAAGATTGTTGG GTCGCTTTTTTT$_v$AATTTCGCGTTCTAACAACC	0.013
D	N-Ada16Δ	CAGCGAAAAAAAT TAAAGCGCAAGATTGTTGG GTCGCTTTTTTTTA$_v$ATTTCGCGTTCTAACAACC	0.041
E	N-Ada16Δ	CA GCGAAAAAAATTAAAGCGCAAGATTGTTGG GT$_v$CGCTTTTTTTTAATTTCGCGTTCTAACAACC	1.3
F	N-Ada16Δ C38G mutant	CAGCGAAAAAAATTAAAGCGCAAGATTGTTGG GTCGCTTTTTTTTAATTTCGCGTTCTAACAACC	0.039

$_v$ represents N-Me phosphoramidate linkage

Figure 7. Removal of Negative Charges in the N-Ada-DNA Interface Stimulates Complex Formation

Shown in (A)–(F) are electrophoretic mobility shift assays using the protein and DNA constructs indicated in the table below. See the text for details.

phosphoramidate at position T2pA3, which lies near Cys38, caused the same gain in affinity (100-fold) of the unmethylated protein as did methylating the protein on unmodified DNA. Introduction of the phosphoramidate at position A3pA4 also stimulated binding by the unmethylated protein, though by a lesser amount than T2pA3 (32-fold). As an alternative strategy, we mutated Cys38 to Gly, thereby replacing the anionic thiolate ligand on zinc with the neutral water ligand. This charge-neutralizing modification of the protein side of the Ada-DNA interface, involving a change other than Cys-methylation, increased the affinity of the protein for DNA by 33-fold. Finally, electrostatic field calculations for both the methylated and unmethylated N-Ada complexes corroborate the notion that a substantial decrease in repulsive electrostatic interaction accompanies methylation of Cys38 (W. Yang, G.L.V, and M. Karplus, unpublished data). Taken together, these data establish that methylation of Ada on Cys38 facilitates protein-DNA association by alleviating repulsive interactions at the interface between the two macromolecules; methylation-dependent transcriptional activation by Ada is thus controlled by a simple electrostatic switch.

Structural Commonality in DNA Repair and Sequence-Specific DNA Recognition by N-Ada

The N-terminal domain of Ada has two distinct functional roles: repair of S_p-configurated methyl phosphotriesters and sequence-specific binding to the promoters of the *ada* regulon. In each instance, N-Ada must perform an efficient search for the presence of some cognate structural feature in DNA, either an aberrant methyl group on the phosphate group of the DNA backbone or a certain pattern of functional groups in the duplex spaced appropriately to establish chemically complementary interactions with the N-Ada$_N$ and N-Ada$_C$. Whereas the search for methyl phosphotriesters should be virtually ignorant of DNA sequence context, that for cognate promoters must be exquisitely attuned to even minor divergence in sequence. The functional duality of N-Ada function thus presents the paradox of whether

the two processes originate from distinct structural foundations or whether there exists some unifying structural feature relating the two. The present structural information suggests a simple model that resolves this paradox.

Our formulation of the present model is strongly influenced by three key features of the structural data. (1) Cys38-methylated N-Ada$_N$ binds to the A box in a way that evokes a structural picture for phosphotriester repair; a nonsequence-specific phosphotriester attack complex could be modeled from the present X-ray structure by merely translocating the methyl group from SMeCys38 to the nearby pro-S$_p$ phosphate oxygen. (2) N-Ada$_C$ transitions between specific and nonspecific DNA binding modes through a relatively modest motion akin to breathing of the domain-DNA interface. (3) N-Ada$_N$ and N-Ada$_C$ make no significant interdomain contacts with each other and are connected by a flexible linker that adopts different conformations depending on how the 2-folded domains interact with the target DNA. Based upon these features, we propose that N-Ada can transition between DNA searching, phosphotriester recognition and repair, and sequence-specific DNA binding modes by modest changes in the N-Ada$_N$-DNA and N-Ada$_C$-DNA interfaces.

How does the protein locate methyl phosphotriesters in DNA? As discussed above, in the absence of methylation, the N-Ada$_N$-DNA interface suffers a repulsive interaction caused by the close juxtaposition of two zinc bound thiolates (on Cys38 and Cys69) with two successive DNA phosphates (Figure 6A). Just as this interfacial repulsion can be mitigated by methylation of Cys38 on N-Ada, so too can it be reduced by methylation of the DNA backbone (Figure 6B), because the resulting phosphotriester is charge neutral. We therefore envision that unmethylated N-Ada glides along the DNA backbone, held mostly by electrostatic forces (Figure 6A). When N-Ada$_N$ encounters a methyl phosphotriester, electrostatic switching allows the domain to clamp tightly on the DNA backbone and perform zinc-mediated nucleophilic attack on the methyl group, resulting in its transfer to the protein (Figure 6B). The pro-R$_p$ oxygen of T2pA3 is hydrogen bonded to the side-chain hydroxyl of Thr34 and projects into a small pocket incapable of accommodating a methyl group (omitted from Figure 5B for reasons of clarity), which suggests that Ada should bind more strongly to S$_p$-configurated methyl phosphotriester than R$_p$. Obviously, there is also discrimination for the S$_p$ configuration in the covalent transfer step. After methyl transfer, the Cys38-methylated protein would again glide along the DNA backbone until it encountered a promoter (Figure 6C), whereupon both N-Ada$_N$ and N-Ada$_C$ would embrace the duplex tightly (Figure 6D). Thus, both the DNA repair and methylation-dependent DNA binding functions of Ada are fundamentally dependent on electrostatic switching as the structural basis for substrate recognition.

Experimental Procedures

Protein Constructs and Oligonucleotides

The solution structure of methylated N-Ada was solved with a construct containing residues 1–139 bound to an 18-mer duplex DNA containing the *ada* promoter sequence. The construct used for crystallization, N-Ada16Δ, consists of Ada residues 1, 2, and 9–139. Further details are available in the Supplemental Data.

Synthesis of Methyl-^{13}C-Thymine Phosphoramidite

The synthesis of methyl-^{13}C-thymine phosphoramidite was followed from the reported literature procedure (Kellenbach et al., 1992) with minor modifications. Further details are available in Supplemental Data.

Sample Preparation

Methylated N-Ada was prepared as described (Myers et al., 1995a) by treating N-Ada with a synthetic single-stranded oligonucleotide bearing a single methyl phosphotriester. The methylation reaction was carried out in the presence of one mole equivalent (relative to protein) of the sequence-specific duplex DNA relative to protein to stabilize the methylated N-Ada by in situ formation of a DNA complex. The single-stranded DNA was removed afterward by buffer exchange using a Centricon 10K cut-off filter (Amicon).

NMR Sample Preparation

Perdeuterated, ^{15}N-labeled N-Ada16 was expressed in minimal media prepared by using 99.9 atom% D_2O and ^{13}C, d_7-glucose as sole carbon source. A uniformly ^{13}C,^{15}N-labeled and 70% deuterated protein sample was generated by overproduction in growth media prepared with 70 atom% D_2O. A sample of deuterated ^{15}N-labeled N-Ada16 containing only Ile δ1, Leu δ1, δ2, and Val γ1, γ2 labeled with ^{13}C was obtained by overproduction in 99.9 atom% D_2O media supplemented with 100 mg/L [3,3′-d_2] ^{13}C α-ketoisovalerate and 100 mg/L [3-d_1] ^{13}C α-ketobutyrate (Cambridge Isotopes) 30 min before induction. Fully deuterated N-Ada16 containing selective ^{13}C labeling of methyl groups of Val, Ile, and Leu residues and selective protonation of Phe and Tyr residues was produced by expression in M9 minimal media (99.9 atom% D_2O) supplemented with 100 mg/L [3,3′-^{13}C]-α-ketoisovalerate, 50 mg/L [3-^{13}C]–α-ketobutyrate 50 mg/L, 100 mg/L Phe, and 100 mg/L Tyr 30 min before induction. All protein concentrations were quantified by UV spectrophotometry, using ϵ_{278nm} = 19,600 mol^{-1}cm^{-1}. Further details are available in the Supplemental Data.

Crystallization, Data Collection, Phasing, and Refinement

Methylated N-Ada16Δ bound to the 17-mer duplex DNA was buffer exchanged into 10 mM Tris-HCl (pH 7.4), 100 mM NaCl, and 5 mM dithiothreitol (DTT) and crystallized by the hanging droplet method using a reservoir solution of 100 mM sodium cacodylate (pH 6.3), 100 mM NaCl, 50 mM magnesium chloride, and 20%–21% PEG 8000. Crystals were cryoprotected in 20% glycerol and frozen in liquid nitrogen. Multiwavelength anomalous diffraction (MAD) data were collected at the 19ID beamline at the Structural Biology Center in APS. The structure was solved by MAD phasing using selenomethionine-substituted protein. Further details are available in the Supplemental Data.

NMR Spectroscopy

NMR experiments were carried out at 30°C on Varian Inova 900 MHz, Varian Inova 750 MHz, and Varian Inova 500 MHz spectrometers equipped with triple resonance probes and a Bruker Avance 500 MHz NMR spectrometer equipped with a cryoprobe. Protein-DNA complex samples with a concentration of ~0.5 mM were used for data collection. Further details are available in the Supplemental Data.

NMR Structure Calculations

Initial structures were generated by using the program DYANA (Güntert et al., 1997) starting from random conformations of protein and B-form DNA. Further molecular dynamics calculations were performed by using the simulated annealing procedure in X-PLOR (Brünger, 1992). Loose hydrogen bond restrains (lower bound, 2.8 Å; upper bound, 4.0 Å) involving arginine-G contacts between the guanidinium Nη atoms and O6/N7 of guanines were introduced during the final stage of refinements. This routine produced 20 final structures with no NOE violations >0.5 Å and no dihedral angle violations >10.0°. Statistics on the NMR ensemble comprising the 20 final

structures are provided in Table 2. Further details are available in the Supplemental Data.

Electrophoretic Mobility Shift Assay

Binding reactions contained 0.01–100 nM protein and 0.1 nM labeled DNA in 40 μl binding buffer (50 mM Tris [pH 8.0], 1 mM EDTA, 5% glycerol, 0.04 mg/ml BSA, 10 mM βME, and 0.1 μg/ml poly [dI·dC]). Reactions were incubated at 20°C for 1 hr. Samples were run on 10% 29:1 polyacrylamide gels made in 44.5 mM Tris, 1 mM EDTA, and 44.5 mM boric acid, final pH 8.3. Further details are available in the Supplemental Data.

MS/MS Peptide Sequencing

Samples of methylated and unmethylated N-Ada16Δ were isolated by SDS-PAGE, excised, and subjected to reduction, carboxyamidomethylation, and digestion with trypsin. The peptides were analyzed by microcapillary reverse-phase HPLC nano-electrospray tandem mass spectrometry (μLC-MS/MS) on a LCQ DECA XP quadrupole ion trap mass spectrometer (ThermoFinnigan). Further details are available in the Supplemental Data.

Supplemental Data

Supplemental Data include Supplemental Experimental Procedures, Supplemental References, and two figures and are available with this article online at http://www.molecule.org/cgi/content/full/20/1/117/DC1/.

Acknowledgments

This research was supported by grants from the National Institutes of Health (NIH) (to G.W. and G.L.V.), National Science Foundation (to G.W.), and a NIH RR grant (to Robert Griffin, MIT). Use of the Argonne National Laboratory Structural Biology Center beam lines at the Advanced Photon Source was made possible by grants from the U.S. Department of Energy, Office of Biological and Environmental Research. J.C. Fromme provided invaluable assistance and advice. We are grateful to the staff of SBC-CAT of the Advanced Photon Source at Argonne National Laboratory, especially Ruslan Sanishvili, for providing valuable advice and assistance. We thank the staff of MacCHESS, in particular Chris Heaton, for assistance with data collection and processing. We thank R. Robinson, J. Neveu, and J. Asara for expert analysis with mass spectrometry. C.H. is supported by Damon Runyon Fellowship DRG-1628 from the Damon Runyon Cancer Research Foundation.

Received: June 3, 2005
Revised: July 29, 2005
Accepted: August 12, 2005
Published: October 6, 2005

References

Akimaru, H., Sakumi, K., Yoshikai, T., Anai, M., and Sekiguchi, M. (1990). Positive and negative regulation of transcription by a cleavage product of Ada protein. J. Mol. Biol. *216*, 261–273.

Allen, J.R., Clark, D.D., Krum, J.G., and Ensign, S.A. (1999). A role for coenzyme M (2-mercaptoethanesulfonic acid) in a bacterial pathway of aliphatic epoxide carboxylation. Proc. Natl. Acad. Sci. USA *96*, 8432–8437.

Appella, E., and Anderson, C.W. (2001). Post-translational modifications and activation of p53 by genotoxic stresses. Eur. J. Biochem. *268*, 2764–2772.

Berreau, L.M., Makowska-Grzska, M.M., and Arif, A.M. (2000). Amide alcoholysis in mononuclear zinc and cadmium complexes ligated by thioether sulfur and nitrogen donors. Inorg. Chem. *39*, 4390–4391.

Blake, P.R., Park, J.B., Adams, M.W.W., and Summers, M.F. (1992). Novel observation of NH-S(Cys) hydrogen-bond-mediated scalar coupling in 113Cd-substituted Rubredoxin from Pyrococcus furiosus. J. Am. Chem. Soc. *114*, 4931–4933.

Brünger, A.T. (1992). X-PLOR 3.1 Manual (New Haven, CT: Yale University Press).

Chen, X., Vinkemeier, U., Zhao, Y., Jeruzalmi, D., Darnell, J.E., Jr., and Kuriyan, J. (1998). Crystal structure of a tyrosine phosphorylated STAT-1 dimer bound to DNA. Cell *93*, 827–839.

Clark-Baldwin, K., Tierney, D.L., Govindaswamy, N., Gruff, E.S., Kim, C., Berg, J., Koch, S.A., and Penner-Hahn, J.E. (1998). The limitation of X-ray absorption spectroscopy for determining the structure of zinc sites in proteins. When is a tetrathiolate not a tetrathiolate? J. Am. Chem. Soc. *120*, 8401–8409.

Demple, B., Sedgwick, B., Robin, P., Totty, N., Waterfield, M.D., and Lindahl, T. (1985). Active site and complete sequence of the suicidal methyltransferase that counters alkylation mutagenesis. Proc. Natl. Acad. Sci. USA *82*, 2688–2692.

Dodd, I.B., and Egan, J.B. (1990). Improved detection of helix-turn-helix DNA-binding motifs in protein sequences. Nucleic Acids Res. *18*, 5019–5026.

Falnes, P.O., Johansen, R.F., and Seeberg, E. (2002). AlkB-mediated oxidative demethylation reverses DNA damage in *Escherichia coli*. Nature *419*, 178–182.

Freiman, R.N., and Tjian, R. (2003). Regulating the regulators. Lysine modifications make their mark. Cell *112*, 11–17.

Friedberg, E.C., Walker, G.C., and Siede, W. (1995). DNA repair and mutagenesis (Washington, D.C.: ASM Press).

Güntert, P., Mumenthaler, C., and Wüthrich, K. (1997). Torsion angle dynamics for NMR structure calculation with the new program DYANA. J. Mol. Biol. *273*, 283–298.

Hanover, J.A. (2001). Glycan-dependent signaling: O-linked N-acetylglucosamine. FASEB J. *15*, 1865–1876.

Hightower, K.E., and Fierke, C.A. (1999). Zinc-catalyzed sulfur alkylation; insights from protein farnesyltransferase. Curr. Opin. Chem. Biol. *3*, 176–181.

Hunter, T., and Karin, M. (1992). The regulation of transcription by phosphorylation. Cell *70*, 375–387.

Kalodimos, C.G., Biris, N., Bonvin, A.M.J.J., Levandoski, M.M., Guennuegues, M., Boelens, R., and Kaptein, R. (2004). Structure and flexibility adaptation in nonspecific and specific protein-DNA complexes. Science *305*, 386–389.

Karin, M., and Hunter, T. (1995). Transcriptional control by protein phosphorylation: signal transmission from the cell surface to the nucleus. Curr. Biol. *5*, 747–757.

Kellenbach, E.R., Remerowski, M.L., Eib, D., Boelens, R., van der Marel, G.A., van den Elst, H., van Boom, J.H., and Kaptein, R. (1992). Synthesis of isotope labeled oligonucleotides and their use in an NMR study of a protein-DNA complex. Nucleic Acids Res. *20*, 653–657.

Kwon, H.J., Bennik, M.H.J., Demple, B., and Ellenberger, T. (2000). Crystal structure of the *Escherichia coli* Rob transcription factor in complex with DNA. Nat. Struct. Biol. *7*, 424–430.

Landini, P., and Volkert, M.R. (1995a). RNA polymerase alpha subunit binding site in positively controlled promoters: a new model for RNA polymerase-promoter interaction and transcriptional activation in the *Escherichia coli* ada and aidB genes. EMBO J. *14*, 4329–4335.

Landini, P., and Volkert, M.R. (1995b). Transcriptional activation of the *Escherichia coli* adaptive response gene aidB is mediated by binding of methylated Ada protein. Evidence for a new consensus sequence for Ada-binding sites. J. Biol. Chem. *270*, 8285–8289.

Landini, P., and Busby, S.J.W. (1999). The *Escherichia coli* Ada protein can interact with two distinct determinants in the sigma70 subunit of RNA polymerase according to promoter architecture: indentification of the target of Ada activation at the alkA promoter. J. Biol. Chem. *181*, 1524–1529.

Laskowski, R.J., Macarthur, M.W., Moss, D.S., and Thornton, J.M. (1993). PROCHECK: a program to check the stereochemical quality of protein structures. J. Appl. Crystallogr. *26*, 283–290.

LeClerc, G.M., and Grahame, D.A. (1996). Methylcobamide: coenzyme M methyltransferase isozymes from *Methanosarcina barkeri*. J. Biol. Chem. *271*, 18725–18731.

Lin, Y., Dötsch, V., Wintner, T., Peariso, K., Myers, L.C., Penner-Hahn, J.E., Verdine, G.L., and Wagner, G. (2001). Structural basis for the functional switch of the *E. coli* Ada protein. Biochemistry *40*, 4261–4271.

Lindahl, T., Sedgewick, B., Sekiguchi, M., and Nakabeppu, Y. (1988). Regulation and expression of the adaptive response to alkylating agents. Annu. Rev. Biochem. *57*, 133–157.

Luisi, B.F., Xu, W.X., Otwinowski, Z., Freedman, L.P., Yamamoto, K.R., and Sigler, P.B. (1991). Crystallographic analysis of the interaction of the glucocorticoid receptor with DNA. Nature *352*, 497–505.

Matthews, R.G., and Goulding, C.W. (1997). Enzyme-catalyzed methyl transfer to thiols: the role of zinc. Curr. Opin. Chem. Biol. *1*, 332–339.

Maynard, A.T., and Covell, D.G. (2001). Reactivity of zinc finger core: analysis of protein packing and electrostatic screening. J. Am. Chem. Soc. *123*, 1047–1058.

Myers, L.C., Terranova, M.P., Nash, H.M., Markus, M.A., and Verdine, G.L. (1992). Zinc binding by the methylation signaling domain of the *Escherichia coli* Ada protein. Biochemistry *31*, 4541–4547.

Myers, L.C., Terranova, M.P., Ferentz, A.E., Wagner, G., and Verdine, G.L. (1993). Repair of DNA methylphosphotriester through a metalloactivated cysteine nucleophile. Science *261*, 1164–1167.

Myers, L.C., Jackow, F., and Verdine, G.L. (1995a). Metal dependence of transcriptional switching in *Escherichia coli* Ada. J. Biol. Chem. *270*, 6664–6670.

Myers, L.C., Wagner, G., and Verdine, G.L. (1995b). Direct activation of the methyl chemosensor protein N-Ada by CH_3I. J. Am. Chem. Soc. *117*, 10749–10750.

Nicholls, A., Sharp, K.A., and Honig, B. (1991). Protein folding and association: insights from the interfacial and thermodynamic properties of hydrocarbons. Proteins *11*, 281–296.

Ninfa, A.J., and Magasanik, B. (1986). Covalent modification of the glnG product, NRI, by the glnL product, NRII, regulates the transcription of the glnALG operon in Escherichia coli. Proc. Natl. Acad. Sci. USA *83*, 5909–5913.

Radhakrishnan, I., Perez-Alvarado, G.C., Parker, D., Dyson, H.J., Montminy, M.R., and Wright, P.E. (1997). Solution structure of the KIX domain of CBP bound to the transactivation domain of CREB: a model for activator:coactivator interactions. Cell *91*, 741–752.

Rhee, S., Martin, R.G., Rosner, J.L., and Davies, D.R. (2000). A novel DNA-binding motif in MarA: the first structure for an AraC family transcriptional activator. Proc. Natl. Acad. Sci. USA *95*, 10413–10418.

Sakashita, H., Sakuma, T., Ohkubo, T., Kainosho, M., Sakumi, K., Sekiguchi, M., and Morikawa, K. (1993). Folding topology and DNA binding of the N-terminal fragment of Ada protein. FEBS Lett. *323*, 252–256.

Sakumi, K., and Sekiguchi, M. (1989). Regulation of expression of the *ada* gene controlling the adaptive response: interactions with the *ada* promoter of the Ada protein and RNA polymerase. J. Mol. Biol. *205*, 373–385.

Sedgwick, B., Robins, P., Totty, N., and Lindahl, T. (1988). Functional domains and methyl acceptor sites of the *Escherichia coli* Ada protein. J. Biol. Chem. *263*, 4430–4433.

Sterner, D.E., and Berger, S.L. (2000). Acetylation of histones and transcription-related factors. Microbiol. Mol. Biol. Rev. *64*, 435–459.

Storek, M.J., Ernst, A., and Verdine, G.L. (2002). High-resolution footprinting of sequence-specific protein-DNA contacts. Nat. Biotechnol. *20*, 183–186.

Teo, I., Sedgwick, B., Kilpatrick, M.W., McCarthy, T.V., and Lindahl, T. (1986). The intracellular signal for induction of resistance of alkylating agents in *E. coli*. Cell *45*, 315–324.

Trewick, S.C., Henshaw, T.F., Hausinger, R.P., Lindahl, T., and Sedgwick, B. (2002). Oxidative demethylation by *Escherichia coli* AlkB directly reverts DNA base damage. Nature *419*, 174–178.

Viadiu, H., and Aggarwal, A.K. (2000). Structure of BamHI bound to nonspecific DNA: a model for DNA sliding. Mol. Cell *5*, 889–895.

Wilker, J.J., and Lippard, S.J. (1997). Alkyl transfer to metal thiolates: kinetics, active species identification, and relevance to the DNA methyl phosphotriester repair center of *Escherichia coli* Ada. Inorg. Chem. *36*, 969–978.

Wood, R.D., Mitchell, M., Sgouros, J., and Lindahl, T. (2001). Human DNA repair genes. Science *291*, 1284–1289.

Accession Numbers

The Protein Data Bank accession number for the crystal structure is 1U8B and for the NMR structure is 1ZGW. The BiomagRes (BMRB) accession number for the NMR data is 6605.